Journal of Alloys and Compounds 509 (2011) 2238–2242

Contents lists available at ScienceDirect

Journal of Alloys and Compounds

journal homepage: www.elsevier.com/locate/jallcom

Novel hybrid proton exchange membrane electrolytes for medium temperature non-humidified fuel cells

G. Lakshminarayana [a], Masayuki Nogami [a,*], I.V. Kityk [b]

[a] Department of Materials Science and Engineering, Nagoya Institute of Technology, Showa, Nagoya 466-8555, Japan
[b] Electrical Engineering Department, Czestochowa Technological University, Al. Armii Krajowej 17, Czestochowa, Poland

ARTICLE INFO

Article history:
Received 25 July 2010
Received in revised form 23 October 2010
Accepted 28 October 2010
Available online 10 November 2010

Keywords:
Inorganic–organic hybrids
Conductivity
H_2/O_2 fuel cells

ABSTRACT

New composite membranes consisting of phosphosilicate (P_2O_5–SiO_2) content and 1-ethyl-3 methylimidazolium tetrafluoroborate [$EMIMBF_4$] ionic liquid were fabricated by sol–gel process. For all the prepared hybrid membranes, the interaction between the doped "hydrophilic" [$EMIMBF_4$] ionic liquid and the inorganic phosphosilicate network was investigated by Fourier transform infrared spectroscopy.

Average pore sizes and specific surface areas were investigated by the Brunauer–Emmett–Teller (BET) method. Thermogravimetry (TG) and differential thermal analysis (DTA) measurements confirmed that the hybrid membranes were thermally stable up to 220 °C. Relatively a high conductivity of 1×10^{-2} S/cm (8.9×10^{-3} S/cm for 40 wt% IL doped 60TMOS–30VTMOS–10PO$(OCH_3)_3$ (mol%) hybrid membrane) was obtained for 40 wt% IL doped 30TMOS–30TEOS–30MTEOS–10PO$(OCH_3)_3$ hybrid membrane, at 155 °C under anhydrous conditions. The hydrogen permeability was found to decrease within the range 10^{-11} to 10^{-12} mol/cm s Pa for 40 wt% IL doped membranes as the temperature increases from 20 to 150 °C.

1. Introduction

Proton exchange membrane fuel cells (PEMFCs), which electrochemically convert the chemical energy of a fuel, e.g., hydrogen, directly into electrical energy are one of the most promising clean energy technologies and suitable primary power source for transportation and stationary applications due to their high conversion efficiency, high power density, and benign environmental impact [1–3]. Nafion®-based perflourosulfonated ionomer membranes are among the commonly employed candidates for PEMFC due to their high and selective permeability for small cations, especially for protons. But they have severe drawbacks, namely cost and environmental issues and limitation of the operation temperature to below 100 °C. In addition, Nafion® and other perfluorinated sulphonic acid membranes suffer from low conductivity at low water contents or high temperatures, relatively low mechanical strength, low stability and high methanol crossover at higher temperatures [4,5].

On the other hand, operation of PEMFCs at high temperatures (>100 °C) provides a number of technological benefits, including higher tolerance to significant quantities of CO, fast electrode kinetics, and no cathode flooding [6–9]. Therefore, in recent years much research has been focused on the development of anhydrous membrane electrolytes with high proton conductivity at temperatures above 100 °C [10–14].

The organosiloxane-based inorganic–organic hybrid materials prepared from organoalkoxysilanes are promising candidates for the proton conducting electrolytes due to the thermal stability and flexibility of organosiloxane networks and the excellent processing versatility [14,15]. The thermal stability of membrane could be improved by the higher dissociation energy of Si–O bond than that of C–C bond [14–16]. The sol–gel technology makes it possible to incorporate organic molecules into an inorganic network, so that they can be combined virtually at any ratio on the molecular level with the formation of hybrid organic–inorganic materials [17,18].

There are several parameters which influence the hydrolysis and condensation reactions (sol–gel process), including the activity of metal alkoxide, water/alkoxide ratio, solution pH, temperature, and nature of the solvent and additive.

One of the various approaches used to develop anhydrous proton exchange membranes above 100 °C was by replacing water as the proton solvent with a liquid that has a higher boiling point [19]. Recently, ionic liquids (ILs), also known as room temperature molten salts, which generally have melting points below 100 °C, have attracted much attention because of their unique properties related to negligible vapor pressure, high chemical, thermal and electrochemical stability, high ionic conductivity, low toxicity, and the ability to dissolve a wide range of organic and inorganic materials [20,21]. The chemical and physical properties of ionic liquids can be varied by carefully choosing the cation and anion from among numerous possibilities. The above unique properties of ionic liquids make them suitable candidates as advanced electrolyte materials in

* Corresponding author. Tel.: +81 52 735 5285; fax: +81 52 735 5285.
E-mail address: nogami@nitech.ac.jp (M. Nogami).

0925-8388/$ – see front matter © 2010 Elsevier B.V. All rights reserved.
doi:10.1016/j.jallcom.2010.10.192

lithium ion batteries [22,23], fuel cells [24,25], double-layer capacitors [26,27], dye-sensitive solar cells [28,29] and actuators [30,31].

In the present work, we report on the fabrication of hybrid membranes using tetraethoxysilane (TEOS)/tetramethoxysilane (TMOS)/methyltriethoxysilane (MTEOS)/vinyltrimethoxysilane (VTMOS)/trimethyl phosphate ($PO(OCH_3)_3$) and 1-ethyl-3 methylimidazolium tetrafluoroborate ($EMIMBF_4$) ionic liquid as sol–gel precursors, and the anhydrous conductivity of these composites is measured.

2. Experimental

2.1. Preparation and characterization of hybrid membranes

The hybrid membranes were prepared by using tetraethyl orthosilicate ($Si(OC_2H_5)_4$, TEOS, 99.9%, Colcote, Japan), tetramethoxysilane ($Si(OCH_3)_4$, TMOS, 99.9%, Colcote, Japan), methyltriethoxysilane (MTEOS, 98%, Aldrich Chemical Com.), vinyltrimethoxysilane ($C_5H_{12}O_3Si$, VTMOS, 99%, Aldrich Chemical Com.), trimethyl phosphate ($PO(OCH_3)_3$, 98%, Colcote, Japan), and [1-ethyl-3-methylimidazolium tetrafluoroborate] (($EMIMBF_4$), 99%, Aldrich Chemical Com.) ionic liquid as precursors. Several compositions of [TMOS–TEOS–MTEOS–$PO(OCH_3)_3$–IL (i.e., 30TMOS–30TEOS–30MTEOS–10$PO(OCH_3)_3$–x [$EMIMBF_4$] (x = 10, 20, 30, and 40 wt%)], and [TMOS–VTMOS–$PO(OCH_3)_3$–IL (i.e., 60TMOS–30VTMOS–10$PO(OCH_3)_3$–x [$EMIMBF_4$] (x = 10, 20, 30, and 40 wt%)] were selected for the ionic liquid content optimization. Here, "x" is the ratio of the weight of IL to the total weight of the sample. The present hybrid membranes preparation procedure is similar to our recent reports [32–34], except the different selected chemical precursors. All the prepared membranes structural, thermal properties and anhydrous conductivity were studied with the usual equipments as reported earlier [32–34].

3. Results and discussion

Fig. 1 presents the FT-IR spectra of 40 wt% ionic liquid doped hybrid membranes including host phosphosilicate matrices. For 30TMOS–30TEOS–30MTEOS–10$PO(OCH_3)_3$ (mol%) host matrix, several spectral peaks centered at 3628, 3436, 2362, 1664, 1466, 1279, 1148, 1054, 955, 850, 799, 580, and 435 cm^{-1} are identified. Similarly, for 60TMOS–30VTMOS–10$PO(OCH_3)_3$ (mol%) host matrix, spectral bands at 3647, 3293, 2964, 2863, 2360, 2342, 1698, 1605, 1472, 1413, 1137, 1058, 972, 858, 778, 723, 699, 675, 669, 645, 621, 614, 591, 584, 577, 560, 554, 537, 530, 524, 507, 500, 447, 441, 434, 411, and 404 cm^{-1} are found. On the other hand, absorption bands centered at 3846, 3738, 3479, 3468, 3436, 3413, 3401, 2361, 2342, 1637, 1575, 1542, 1508, 1458, 1430, 1337, 1278, 1170, 1124, 1084, 834, 800, 756, 670, 650, 622, 601, 594, 533, 523, and 454 cm^{-1} are identified for 30TMOS–30TEOS–30MTEOS–10$PO(OCH_3)_3$ (mol%) membrane doped with 40 wt% [$EMIMBF_4$] ionic liquid (Fig. 1, curve (a)). Similarly, spectral bands centered at 3823, 3738, 3436, 3154, 3100, 2360, 2342, 1637, 1573, 1458, 1412, 1334, 1278, 1169, 1124, 1084, 770, 723, 715, 700, 692, 684, 676, 669, 646, 622, 533, 523, 509, 456, and 411 cm^{-1} are found for 60TMOS–30VTMOS–10$PO(OCH_3)_3$ (mol%) membrane doped with 40 wt% [$EMIMBF_4$] ionic liquid (Fig. 1, curve (b)). All these identified spectral bands correlate well with the pure [$EMIMBF_4$] ionic liquid absorption bands [35]. Table 1 shows all the relevant observed FTIR bands with assignment.

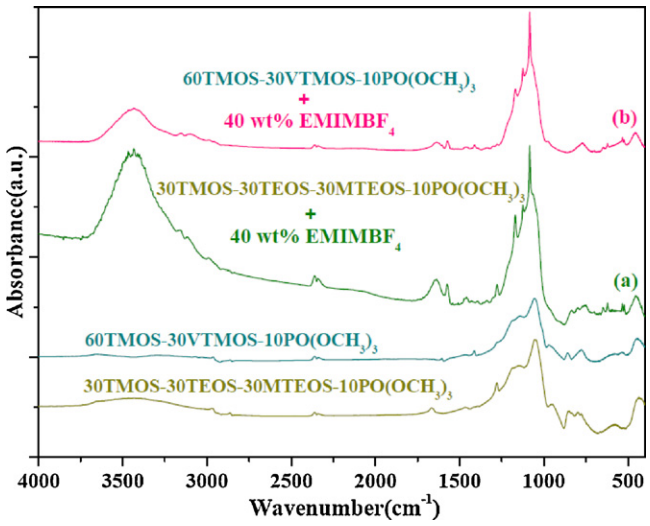

Fig. 1. FT-IR spectra of 30TMOS–30TEOS–30MTEOS–10PO $(OCH_3)_3$–x [$EMIMBF_4$] (x = 0, 40 wt% (curve a)); 60TMOS–30VTMOS–10$PO(OCH_3)_3$–x [$EMIMBF_4$] (x = 0, 40 wt%(curve b)) hybrid membranes.

For the ionic liquid based membranes, within the wavenumber range 400–1200 cm^{-1}, phosphosilicate matrix related spectral bands were overlapped with the ionic liquid bands. The above results indicate that in the prepared hybrid membranes the [$EMIMBF_4$] ionic liquid interact effectively with phosphosilicate content. Because of the physico-chemical properties including low viscosity, and high ionic conductivity; [$EMIMBF_4$] ionic liquid is expected to be a useful solvent for electrochemical studies in the absence of water.

Fig. 2 shows the pore size distribution curves for both the 40 wt% IL doped hybrid membranes. Table 2 presents the pore sizes and surface area properties for all the hybrid membranes, prepared in the present work. Following the data presented in Table 2, a

Table 1
FTIR spectral bands with assignments.

Band position (cm^{-1})	Assignment [Ref. [32–35]]
400–880	Si–O–Si bond bending vibrations and symmetric stretching vibrations of Si–O–Si bonds
799, 778	Symmetric stretching of the P–O–P and Si–O–Si (bridging oxygen atoms between the tetrahedral) bonds
955	Stretching vibration of free silanol groups on the surface of the amorphous silica
1054, 1058	ν_{as} Si–O–Si (TO mode) vibrations
1137	P–O–Si bridging units
1148, 1279	Asymmetric stretching vibrations of Si–O–Si bridging sequences, and O=P bond stretching
1664	Bending modes of the interstitial water molecules
1640–1960	Combination of vibrations of the SiO_2 network, molecular water band
3293	Silanol groups linked to molecular water through hydrogen bonds
3628, 3436	Pair of surface Si–OH groups that are mutually linked by hydrogen bond or internal Si–OH bonds; and silanol groups linked to molecular water through hydrogen bonds
3500–3750	OH stretching band
3000–4000	Overtones or combinations of vibrations of Si–OH or H_2O
For [$EMIMBF_4$] ionic liquid doped hybrids	
500–850	Out-plane C–H bending vibrations of imidazolium ring
1030–1090	Asymmetric stretching vibrations of BF_4^-
1150–1650	Unresolved CH_3–N stretching vibration, CH_2–N stretching vibration, and ring in plane asymmetric stretching, and C–C stretching vibrations of the imidazolium ring
2900–3750	C–N, C–H stretching vibration modes of the imidazolium ring
2359, 2342	Atmospheric CO_2

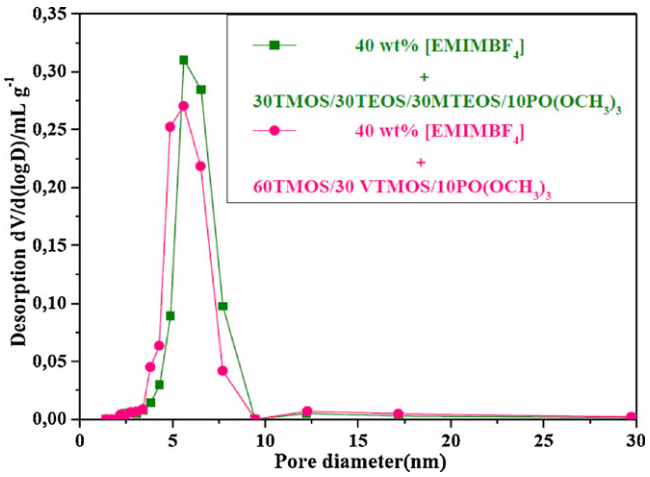

Fig. 2. Pore size distribution curves of both the 40 wt% IL doped hybrid membranes.

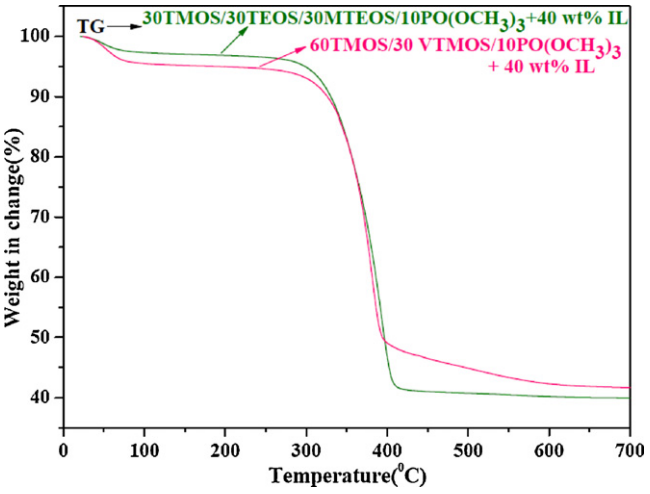

Fig. 3. TGA profiles of both the 40 wt% IL doped hybrid membranes.

decrease in specific surface area and pore volume, and an increase in the pore size is observed for all the IL doped hybrid membranes. The decrement in surface area could be due to an increase of the IL domains in the interconnected phosphosilicate inorganic network.

As the present membranes are being developed as medium temperature proton conducting membranes to be used in PEMFCs at 150 °C, so they should be thermally stable up to higher temperatures. The thermal stability of all the prepared membranes was studied and Fig. 3 shows the thermogravimetric analysis (TGA) mass loss curves for both the 40 wt% IL doped hybrid membranes.

The temperature of weight loss by 5% and 10% for all the prepared membranes was determined from the measured TGA curves and is listed in Table 3.

All the IL doped hybrid membranes were thermally stable up to 200 °C without any weight loss. Also the dissociation temperature corresponding to 5 and 10% weight loss is above 200 °C for all the IL doped hybrid membranes (Table 3), which indicates that these membranes can be used in the medium temperature (100–150 °C) fuel cells. It should be emphasized that thermal stability tests in our present study measured by the TGA method do not reflect that real thermal stability of the IL as well as membrane electrolytes when they are kept at elevated temperatures, but the present characterization gives us an idea of the thermal stability of the membranes.

Fig. 4(a) shows the Cole–Cole representation of impedance data measured for 40 wt% IL doped membrane at 85 and 155 °C, respectively. Under non-humidified conditions, the Cole–Cole plots showed the semicircle component at high frequencies. Generally, the impedance arcs in high frequency region represent bulk properties of the material [36], which in our case is the proton conductivity. The semicircle at high frequency can be explained with the capacitive behavior of the interface between electrodes and electrolyte. However, this component has decreased with the increase of membrane conductivity. Increasing temperature leads to smaller semicircles due to reducing resistance because proton conductivity is in general a thermally stimulated process.

In PEMFCs, conductivity of membranes is a crucial parameter because the cell performance is strongly dependent on this property. Fig. 4(b) presents the conductivity of both the 40 wt% IL doped hybrid membranes within the temperature range −25 to −155 °C. Inset plot shows the variation of conductivity with IL weight ratio. The thickness of all the prepared hybrid membranes for the conductivity measurements was about 0.2 mm. The doped ionic liquid was expected to act as a proton transporting medium in the membranes as water does for water-swollen proton conducting membranes operated below 100 °C. For all the IL doped hybrid membranes, conductivity was increased with an increase in the IL weight percent ratio from 10 to 40 wt%. The temperature effect on the conductivity results form two possible reasons. First, with the increase in temperature, the decreased viscosity of ionic liquid facilitates its mobility and accordingly enhances the proton transporting process inside the membrane. Second, the ionic conductivity of $EMIMBF_4$ itself also increases with the temperature. Generally, the conductivity of the membranes containing hydrophilic ILs ($EMIMBF_4$ or $BMIMBF_4$) is higher than that of the membranes containing hydrophobic ILs ($EMIMPF_6$ or $BMIMPF_6$) [37]. Maximum anhydrous conductivity of 10 mS/cm, and 8.9 mS/cm at 155 °C was measured for 40 wt% IL doped membranes, respectively. However, the conductivity of these ionic liquid based composite membranes is lower than that of the original [$EMIMBF_4$] ionic liquid, which is also observed in other hybrid membranes doped with ionic liquids [38].

Table 2
Textural properties of [30TMOS–30TEOS–30MTEOS–10($PO(OCH_3)_3$)–*x* [$EMIMBF_4$] (*x* = 0, 10, 20, 30, and 40 wt%)], and [60TMOS–30VTMOS–10($PO(OCH_3)_3$)–*x* [$EMIMBF_4$] (*x* = 0, 10, 20, 30, and 40 wt%)] membranes.

Sample	Composition of TMOS–TEOS–MTEOS–$PO(OCH_3)_3$)–*x* [$EMIMBF_4$]	Average pore size (nm)	Average pore volume (cm^3/g)	Specific surface area (m^2/g)
S1	(30–30–30–10)–0 wt%	1.039	0.00047	1.83
S2	(30–30–30–10)–10 wt%	5.927	0.065	44.24
S3	(30–30–30–10)–20 wt%	8.275	0.1077	52.06
S4	(30–30–30–10)–30 wt%	7.691	0.0544	28.29
S5	(30–30–30–10)–40 wt%	9.619	0.0517	21.49
	Composition of TMOS-VTMOS-$PO(OCH_3)_3$)–*x* [$EMIMBF_4$]			
S6	(60–30–10)–0 wt%	2.55	0.0548	86.065
S7	(60–30–10)–10 wt%	5.145	0.0984	76.48
S8	(60–30–10)–20 wt%	9.523	0.0666	27.99
S9	(60–30–10)–30 wt%	10.14	0.0551	21.11
S10	(60–30–10)–40 wt%	10.44	0.0527	20.78

Table 3
TGA data for all the prepared hybrid membranes including host phosphosilicate membranes.

Sample	Composition of TMOS–TEOS–MTEOS–$PO(OCH_3)_3$)–*x* [$EMIMBF_4$]	Temperature at 5 and 10 wt% loss	
		$T_{d5\%}$ (°C)	$T_{d10\%}$ (°C)
S1	(30–30–30–10)–0 wt%	215	522
S2	(30–30–30–10)–10 wt%	290	326
S3	(30–30–30–10)–20 wt%	311	339
S4	(30–30–30–10)–30 wt%	311	338
S5	(30–30–30–10)–40 wt%	299	330
	Composition of TMOS–VTMOS–$PO(OCH_3)_3$)–*x* [$EMIMBF_4$]		
S6	(60–30–10)–0 wt%	88	346
S7	(60–30–10)–10 wt%	221	314
S8	(60–30–10)–20 wt%	232	317
S9	(60–30–10)–30 wt%	234	321
S10	(60–30–10)–40 wt%	230	326

Further from Fig. 4(b), it is observed that the plots of conductivity (σ) versus reciprocal temperature (T^{-1}) are not linear which indicates that conduction in the IL doped membranes does not exactly follow an Arrhenius-type relation, but also exhibits the Vogel–Tamman–Fulcher (VTF) type behavior [39].

Practically, a good membrane must allow less hydrogen molecules diffusing through its matrix. Otherwise, the PEMFC will loss the hydrogen supplied before it is dissociated to protons. The hydrogen permeability through the prepared 40 wt% IL doped membranes was measured under constant input pressure. Fig. 5 presents the measured hydrogen permeability values for both the 40 wt% IL doped hybrid membranes within the temperature range 20–150 °C (thickness = 0.5 mm). The hydrogen permeability values were decreased from 1.41×10^{-11} to 0.1×10^{-12} mol/cm s Pa, and 1.38×10^{-11} to 0.3×10^{-12} mol/cm s Pa, respectively for these hybrid membranes with temperature increment from 20 to 150 °C. It is well known that the permeability coefficient of any pure gas through a membrane electrolyte depends on size and thickness of the membrane including applied gas pressure. To enhance the power density, decrease of the membrane interfacial resistance by means of reduction of the thickness of the electrolyte membrane is required without loss of mechanical strength.

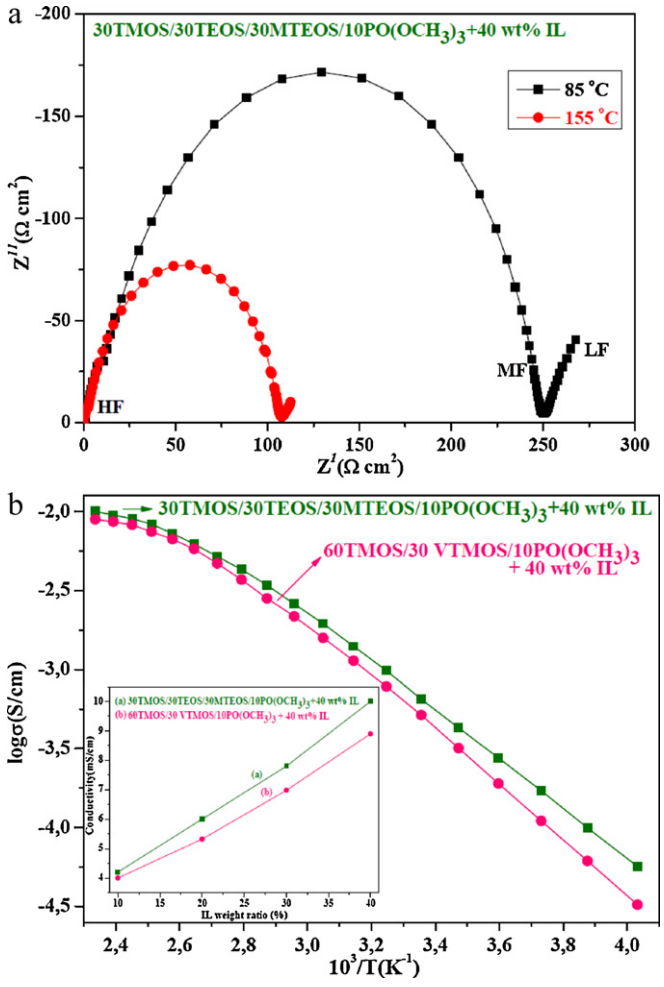

Fig. 4. (a) Cole–Cole representation of impedance data measured at 85, and 155 °C for 40 wt% IL doped hybrid membrane and (b) conductivity of both the 40 wt% IL doped hybrid membranes, and variation of conductivity with IL weight ratio at 155 °C (inset plot).

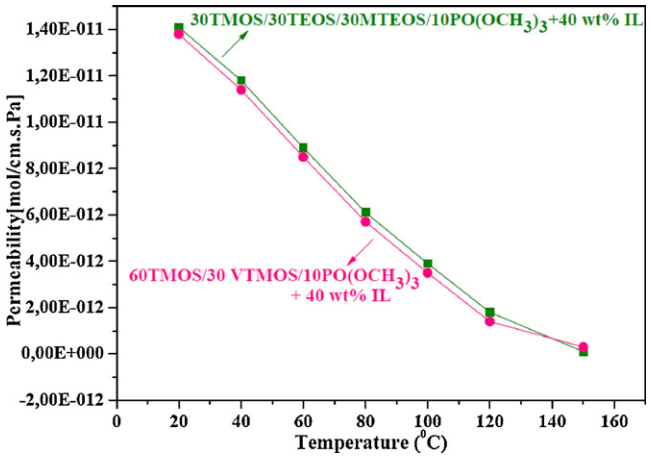

Fig. 5. Hydrogen permeation rate as a function of temperature for both the 40 wt% IL doped hybrid membranes.

4. Conclusions

[$EMIMBF_4$] ionic liquid based inorganic–organic hybrid phosphosilicate membranes were successfully prepared by sol–gel process through hydrolysis and condensation of TMOS, TEOS, MTEOS, VTMOS and $PO(OCH_3)_3$, respectively. These hybrid membranes possess good chemical stability and are thermally stable up to 220 °C in air due to inorganic SiO_2 framework and stable [BF_4] anion. The average pore sizes were increased proportionally with the ionic liquid weight percent ratio in the phosphosilicate matrices within the range 1–9.6 nm (2.55–10.44 nm for all 60TMOS–30VTMOS–10$PO(OCH_3)_3$ (mol%) hybrid membranes) for all 30TMOS–30TEOS–30MTEOS–10$PO(OCH_3)_3$ hybrid membranes, respectively. Maximum anhydrous conductivity of 1×10^{-2} S/cm was obtained for 40 wt% IL doped 30TMOS–30TEOS–30MTEOS–10$PO(OCH_3)_3$ hybrid membrane, at 155 °C under anhydrous conditions. Similarly, for 40 wt% IL doped

60TMOS–30VTMOS–10PO$(OCH_3)_3$ (mol%) hybrid membrane, conductivity of 8.9×10^{-3} S/cm was measured at 155 °C, under non-humidified conditions. The hydrogen permeability was found to decrease within the range 10^{-11} to 10^{-12} mol/cm s Pa for 40 wt% IL doped membranes as the temperature increases from 20 to 150 °C. The prepared IL doped hybrid membranes are suitable for potential use in proton exchange membrane fuel cells (PEMFCs) at medium temperatures (100–150 °C) under non-humidified conditions.

Acknowledgments

The authors are grateful to the New Energy and Industrial Technology Development Organization (NEDO), Japan for the financial support.

References

[1] M. Monroy-Barreto, J.L. Acosta, C. del Río, M.C. Ojeda, M. Muñoz, J.C. Aguilar, E. Rodríguez de San Miguel, J. de Gyves, J. Power Sources 195 (2010) 8052–8060.
[2] W.-M. Yan, X.-D. Wang, D.-J. Lee, X.-X. Zhang, Y.-F. Guo, A. Su, Appl. Energy 88 (2011) 392–396.
[3] W. Phompan, N. Hansupalak, J. Power Sources 196 (2011) 147–152.
[4] F. Damay, L.C. Klein, Solid State Ionics 162 (2003) 261–267.
[5] S.H. Seo, C.S. Lee, Appl. Energy 87 (2010) 2597–2604.
[6] V.D. Noto, N. Boaretto, E. Negro, G. Pace, J. Power Sources 195 (2010) 7734–7742.
[7] M. Boaventura, M.L. Ponce, L. Brandão, A. Mendes, S.P. Nunes, Int. J. Hydrogen Energy 35 (2010) 12054–12064.
[8] M. Kato, J. Umeda, M. Suzuki, M. Moriya, W. Sakamoto, T. Yogo, in: K. Ewsuk, M. Naito, T. Kakeshita, S. Kirihara, K. Uematsu, H. Abe (Eds.), Characterization and Control of Interfaces for High Quality Advanced Materials III, John Wiley & Sons, Inc., Hoboken, NJ, USA, 2010.
[9] Ş. Özden, S.Ü. Çelik, A. Bozkurt, J. Polym. Sci. A: Polym. Chem. 48 (2010) 4974–4980.
[10] M.B. Herath, S.E. Creager, A. Kitaygorodskiy, D.D. DesMarteau, Chem. Phys. Chem. 11 (2010) 2871–2878.
[11] H. Pu, L. Wang, H. Pan, D. Wan, J. Polym. Sci. A: Polym. Chem. 48 (2010) 2115–2122.
[12] S.-Y. Lee, A. Ogawa, M. Kanno, H. Nakamoto, T. Yasuda, M. Watanabe, J. Am. Chem. Soc. 132 (2010) 764–9773.
[13] U. Sen, A. Bozkurt, A. Ata, J. Power Sources 195 (2010) 7720–7726.
[14] G. Lakshminarayana, V.S. Tripathi, I. Tiwari, M. Nogami, Ionics 16 (2010) 385–395.
[15] M. Kato, W. Sakamoto, T. Yogo, J. Membr. Sci. 303 (2007) 43–53.
[16] Y.-il Park, M. Nagai, Solid State Ionics 145 (2001) 149–160.
[17] J.D. Mackenzie, J. Sol–Gel Sci. Technol. 26 (2003) 23–27.
[18] D. Arcos, M. Vallet-Regí, Acta Biomater. 6 (2010) 2874–2888.
[19] J.C. Padilha, J. Basso, L.G. da Trindade, E.M.A. Martini, M.O. de Souza, R.F. de Souza, J. Power Sources 195 (2010) 6483–6485.
[20] Z. Liu, T. Chen, A. Bell, B. Smit, J. Phys. Chem. B 114 (2010) 4572–4582.
[21] E. Bodo, L. Gontrani, A. Triolo, R. Caminiti, J. Phys. Chem. Lett. 1 (2010) 1095–1100.
[22] M. Nadherna, R. Dominko, D. Hanzel, J. Reiter, M. Gaberscek, J. Electrochem. Soc. 156 (2009) A619–A626.
[23] B. Rezaei, S. Mallakpour, M. Taki, J. Power Sources 187 (2009) 605–612.
[24] E.K. Cho, J.S. Park, S.S. Sekhon, G.G. Park, T.H. Yang, W.Y. Lee, C.S. Kim, S.B. Park, J. Electrochem. Soc. 156 (2009) B197–B202.
[25] V.D. Noto, E. Negro, J.Y. Sanchez, C. Iojoiu, J. Am. Chem. Soc. 132 (2010) 2183–2195.
[26] B. Xu, F. Wu, R. Chen, G. Cao, S. Chen, Y. Yang, J. Power Sources 195 (2010) 2118–2124.
[27] M. Drüschler, B. Huber, S. Passerini, B. Roling, J. Phys. Chem. C 114 (2010) 3614–3617.
[28] L. Guo, X. Pan, C. Zhang, W. Liu, M. Wang, X. Fang, S. Dai, Solar Energy 84 (2010) 373–378.
[29] H.R. Jhong, D.S.H. Wong, C.C. Wan, Y.Y. Wang, T.C. Wei, Electrochem. Commun. 11 (2009) 209–211.
[30] W. Lu, A.G. Fadeev, B. Qi, E. Smela, B.R. Mattes, J. Ding, G.M. Spinks, J. Mazurkiewicz, D. Zhou, G.G. Wallace, D.R. MacFarlane, S.A. Forsyth, M. Forsyth, Science 297 (2002) 983–987.
[31] N. Terasawa, I. Takeuchi, H. Matsumoto, Sens. Actuators B: Chem. 139 (2009) 624–630.
[32] G. Lakshminarayana, M. Nogami, Electrochim. Acta 55 (2010) 1160–1168.
[33] G. Lakshminarayana, M. Nogami, I.V. Kityk, J. Electrochem. Soc. 157 (2010) B892–B899.
[34] G. Lakshminarayana, M. Nogami, Solid State Ionics 181 (2010) 760–766.
[35] D. Wang, Y.-X. Li, Z. Shi, H.-L. Qin, L. Wang, X.-F. Pei, J. Jin, Langmuir 26 (2010) 14405–14408.
[36] C.A. Edmondson, P.E. Stallworth, M.E. Chapman, J.J. Fontanella, M.C. Wintersgill, S.H. Chung, S.G. Greenbaum, Solid State Ionics 135 (2000) 419–423.
[37] H. Tokuda, S. Tsuzuki, M.A.B.H. Susan, K. Hayamizu, M. Watanabe, J. Phys. Chem. B 110 (2006) 19593–19600.
[38] Q. Che, B. Sun, R. He, Electrochim. Acta 53 (2008) 4428–4434.
[39] F. Yan, S. Yu, X. Zhang, L. Qiu, F. Chu, J. You, J. Lu, Chem. Mater. 21 (2009) 1480–1484.